

Mitotic Spindle Regulation by *Nde1* Controls Cerebral Cortical Size

Yuanyi Feng and Christopher A. Walsh*

Department of Neurology
Howard Hughes Medical Institute
Beth Israel Deaconess Medical Center
Harvard Medical School
77 Avenue Louis Pasteur
Boston, Massachusetts 02115

Summary

Ablation of the LIS1-interacting protein *Nde1* (formerly *mNudE*) in mouse produces a small brain (microcephaly), with the most dramatic reduction affecting the cerebral cortex. While cortical lamination is mostly preserved, the mutant cortex has fewer neurons and very thin superficial cortical layers (II to IV). BrdU birth-dating revealed retarded and modestly disorganized neuronal migration; however, more dramatic defects on mitotic progression, mitotic orientation, and mitotic chromosome localization in cortical progenitors were observed in *Nde1* mutant embryos. The small cerebral cortex seems to reflect both reduced progenitor cell division and altered neuronal cell fates. In vitro analysis demonstrated that *Nde1* is essential for centrosome duplication and mitotic spindle assembly. Our data show that mitotic spindle function and orientation are essential for normal development of mammalian cerebral cortex.

Introduction

The development of the cerebral cortex follows a strictly regulated sequence of neuronal proliferation, migration, and differentiation. In all mammalian species, cortical neurons are generated in the proliferative pseudostratified ventricular zone, where neural progenitor cells go through massive expansion before they exit the cell cycle and form cortical neurons (Caviness et al., 1995; Rakic, 1995). Upon finishing the terminal mitotic cell cycle, newly born neurons leave the ventricular zone and move toward the cortical pial surface through a highly ordered process of neuronal migration (Takahashi et al., 1995; Rakic, 1995; Caviness et al., 1995). While terminal differentiation through extensive axonal and dendrite remodeling and networking is completed after neurons arrive at the cerebral cortex, the early proliferation and migration processes determine the number and location of the cortical neurons and are essential for the formation of the laminated functional cerebral cortex (Rakic, 1988a, 1988b).

Disorders of cerebral cortical development are generally categorized by the developmental stage that is disrupted (Barkovich et al., 1996). For example, impaired neurogenesis affects brain size and results in “microcephaly” (small brain) (Bond et al., 2002; Mochida and Walsh, 2001), and defective neuronal migration results

in cortical lamination defects as seen in a variety of cortical malformations (D’Arcangelo et al., 1995; des Portes et al., 1998; Dobyns et al., 1993; Fox et al., 1998; Gleeson et al., 1998; Olson and Walsh, 2002; Reiner et al., 1993; Yoshida et al., 2001). Lissencephaly (smooth brain) is considered to be neuronal migration disorder (Dobyns and Truwit, 1995). In addition to reduced or absent gyri and sulci, lissencephalic brains typically show an abnormally thickened cortex with striking disruption of the normal six-layered neocortical pattern at the histological level (Barkovich et al., 1991; Dobyns et al., 1993). Since many neurons in lissencephalic brains are observed in deeper regions that are normally occupied by glial cells, it has been believed that the disease is primarily caused by a neuronal migration arrest during embryonic development (Kato and Dobyns, 2003).

Heterozygous mutations of the *LIS1* gene in human are known to account for a large fraction of classical, type I lissencephaly (Pilz et al., 1998), and the *LIS1* protein is associated with multiple cellular proteins, including platelet-activating factor acetylhydrolase, microtubules, and dynein motors (Faulkner et al., 2000; Hattori et al., 1995; Sapir et al., 1997; Smith et al., 2000). While these interactions provided important information on the molecular basis of *LIS1* function, many questions regarding the role of *LIS1* in cortical neuronal migration as well as the pathogenic mechanism of lissencephaly remain unanswered. The *LIS1* gene is ubiquitously expressed, and the observation of early embryonic lethality of *LIS1* homozygous mutations in mouse suggests that it is also essential for other cellular functions beyond its role in neuronal migration (Hirotsune et al., 1998). It is still unclear why heterozygous mutations of *LIS1* result in a minimal phenotype in tissues outside of the cerebral cortex. Moreover, the lissencephalic brain is also microcephalic. In addition to neuronal migration defects, *Lis1* compound heterozygous mice also display proliferation defects in cortical neural progenitors (Gambello et al., 2003; Hirotsune et al., 1998). However, the contribution of impaired neurogenesis to the malformation of *LIS1* mutant brain is not yet known.

We previously identified *Nde1* (formerly known as *mNudE*) through its direct physical interaction with *LIS1*, and through its homology with *NUDE*, a genetic suppressor of *LIS1*’s ortholog *NUDF* in the filamentous fungus *A. nidulans* (Efimov and Morris, 2000; Feng et al., 2000b). *Nde1* is localized to the mammalian microtubule organizing center (MTOC, the centrosome) and directs γ -tubulin localization and hence microtubule organization in interphase cells, including cortical neurons (Feng et al., 2000b). In mammals, *Nde1* shares high sequence identity with *Ndel1* (formerly known as *NUDEL*), another homolog of *NUDE* identified through interaction with *LIS1* (Niethammer et al., 2000; Sasaki et al., 2000; Sweeney et al., 2001). While *Ndel1* appears to be more abundant in general, *Nde1* is highly expressed in the developing cerebral cortex in cortical progenitors and young postmitotic neurons (Feng et al., 2000b). Blocking *Nde1*-*LIS1* interactions in *Xenopus* embryos induced a small head and small eye with striking lamination defects, sug-

*Correspondence: cwash@bidmc.harvard.edu

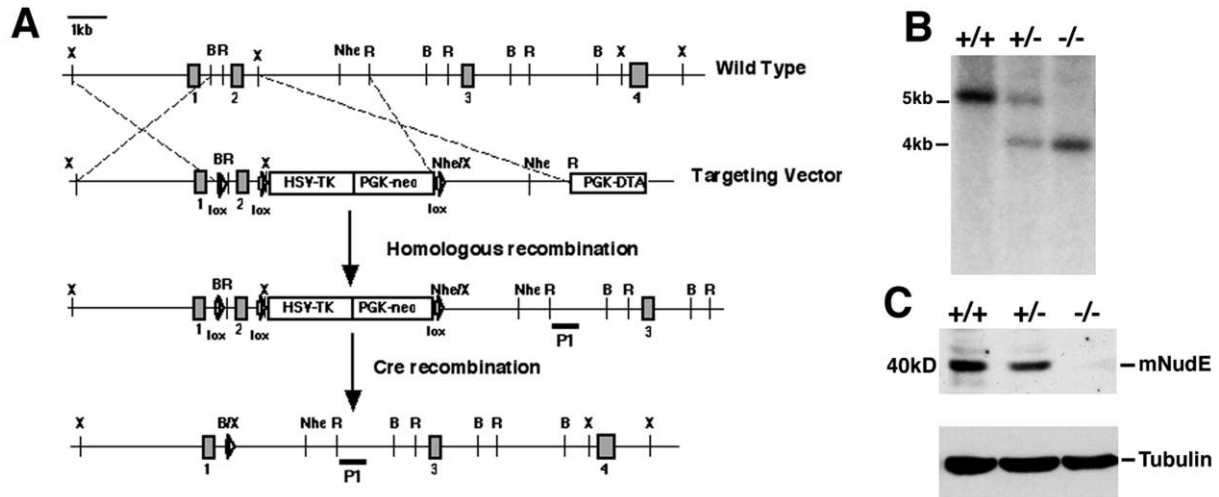


Figure 1. Generation of the *Nde1* Null Mutation through Gene Targeting in Mouse ES Cells

(A) Strategy to generate mice lacking *Nde1* protein. B, BamH1; R, EcoR1; X, Xba1; Nhe, *Nde1*.

(B) Southern blotting with probe P1 of BamH1-digested genomic DNA from wild-type, *Nde1*^{+/-}, and *Nde1*^{-/-} mice, on which the 5.2 kb band represents the wild-type and the 4 kb band represents the exon 2-deleted allele.

(C) Immunoblotting of total protein extracts from E12 wild-type, *Nde1*^{+/-}, and *Nde1*^{-/-} embryos, indicating that deleting exon 2 ablates *Nde1* protein completely.

gesting that *Nde1* mediates LIS1's function in forebrain development. Here, we show that, by organizing mitotic microtubules, *Nde1* is essential for mitotic spindle assembly and function and is required for determining the mode and speed of cortical neural progenitor cell mitosis. Homozygous mutation of *Nde1* in mouse results in a small brain that affects the cerebral cortex preferentially. While homozygous *Nde1* mutant mice showed neuronal migration deficits, mitotic arrest and changes in mitotic orientation were also seen. These mitotic defects led to the failure of neural progenitor pool expansion and alterations in neural cell fate, and they produced a smaller cerebral cortex with dramatically reduced superficial cortical layers. Together, our results demonstrate that *Nde1* plays an essential role in determining the pattern of progenitor cell division and the size of the cerebral cortex.

Results

Nde1 Is Essential for the Development of Cerebral Cortex

We created a *Nde1* null mutation through gene targeting in mouse embryonic stem cells (Figure 1A). By deleting a 1.2 kb genomic region that contains exon 2 of the mouse *Nde1* gene, our targeting strategy yielded a nonsense mutation that truncated the *Nde1* protein at amino acid 27. Southern blotting (Figure 1B) and immunoblotting analysis (Figure 1C) confirmed the predicted genomic deletion and ablation of *Nde1* protein in the homozygous *Nde1* mutant (*Nde1*^{-/-}) mice. Though *Nde1*^{-/-} mice are viable, they show a striking and completely penetrant small-brain phenotype from birth throughout adult life.

Analysis of sixteen 6- to 8-week-old homozygous mutant mice indicated that the *Nde1*^{-/-} brain was one-third smaller by mass than wild-type or heterozygous

counterparts (Figures 2A and 2B). Moreover, the size reduction of the *Nde1* mutant brain predominantly affected the cerebral cortex, while other brain structures, including the hippocampus, the midbrain, and the cerebellum, were either of normal size and structure or only slightly reduced in size (Figures 2B, 2C, 2D, and 2E).

To examine the topography of the brain size reduction of the *Nde1*^{-/-} mice, we compared anterior as opposed to posterior and dorsal as opposed to ventral brain structures in *Nde1*^{-/-} mice and their heterozygous counterparts. *Nde1*^{+/-} and *Nde1*^{-/-} brains were first separated into two parts along the forebrain-midbrain junction (Figure 2F). The mass of the anterior portion, which includes the olfactory bulbs, the cerebrum, and the thalamus, was found to be reduced much more significantly than the posterior structures in the *Nde1*^{-/-} brain compared to their heterozygous counterparts (Figure 2F). Moreover, we compared the area of the dorsal forebrain (the neocortex) to the area of the ventral brain structures (including the basal ganglia, the thalamus, and the hippocampus, as well as the paleocortex) on coronal sections that represented three different levels of the forebrain along the anterior-posterior axis. The results showed that the neocortical area represented by the dorsal to ventral area ratio of *Nde1*^{-/-} brain was significantly smaller in all three levels examined (Figure 2G). In contrast to the greatly reduced cerebral cortex, the basal ganglia in the *Nde1*^{-/-} mutant brain only showed moderate reduction. Together, these data demonstrate that the six-layered neocortex is the most severely affected part in the *Nde1*^{-/-} brain and that *Nde1* is essential for the development of the mammalian cerebral cortex.

Specific Reduction in Upper Cortical Layers Due to *Nde1* Deficiency

Although the brains of *Nde1*^{-/-} mice showed apparently normal overall patterning, the cerebral cortex was con-

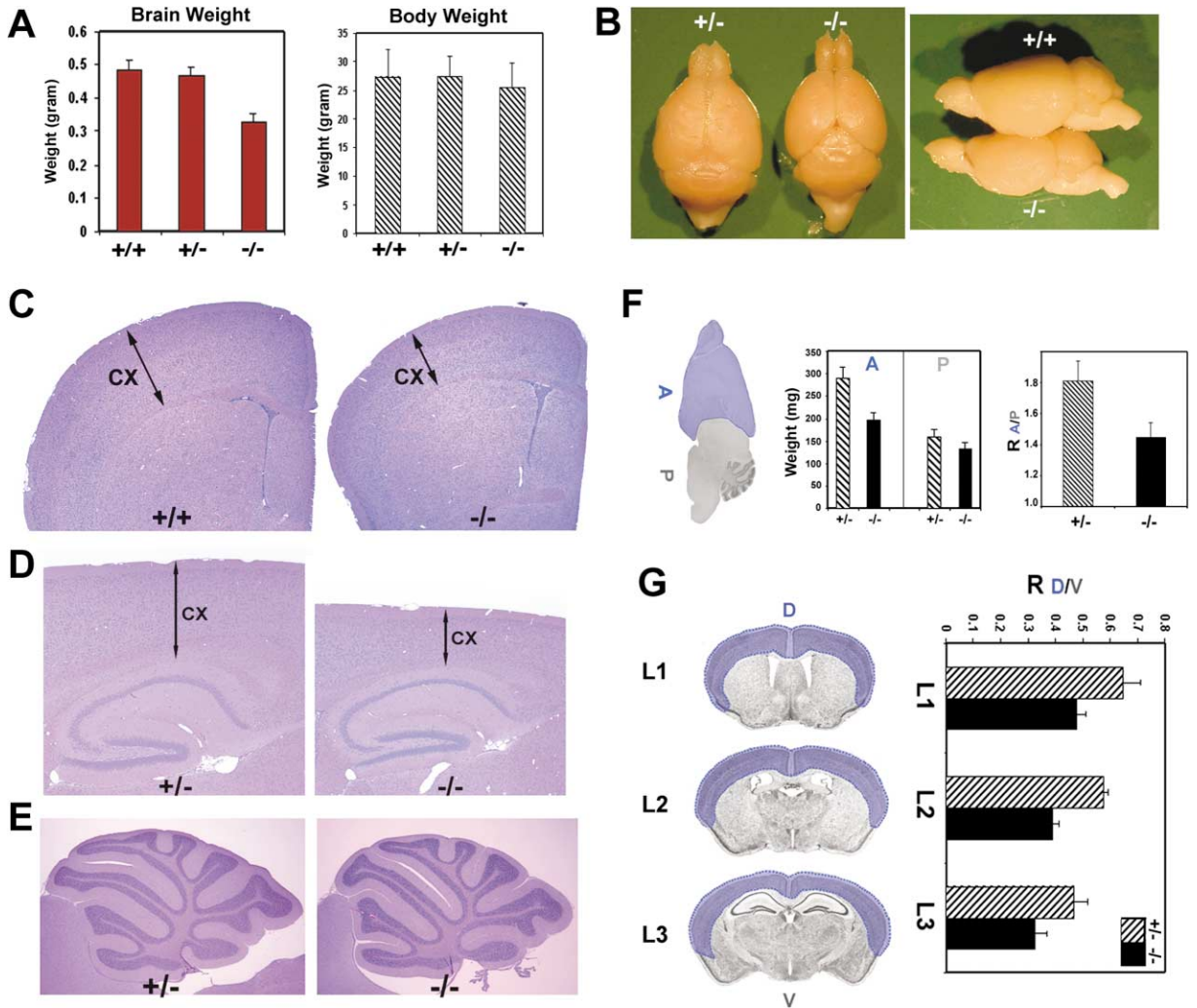


Figure 2. *Nde1* Homozygous Mutation Results in a Reduction in the Size of the Cerebral Cortex

(A) Brain and body weight (mean + SD) of *Nde1*^{-/-} mice (n = 16) and their wild-type (n = 13) and heterozygous (n = 34) littermates at 6–8 weeks, which shows that the *Nde1*^{-/-} brain is significantly lighter than the wild-type and *Nde1*^{+/-} brains in total wet weight (p < 0.0001, by ANOVA F test). In contrast, no significant difference in body weight was detected between the *Nde1*^{-/-} mutants and their wild-type and heterozygous counterparts (p = 0.199, by ANOVA F test).

(B) Dorsal and side views of adult wild-type, *Nde1*^{+/-}, and *Nde1*^{-/-} brains, which show that deleting *Nde1* produces a smaller brain with specific reduction in size and surface area involving the cerebral cortex. In contrast, the cerebellum and the olfactory bulb in the homozygous *Nde1* mutant are much less reduced in size. As a result of the reduced cerebral cortex, the midbrain in homozygous mutants is more exposed and appears larger.

(C) Coronal sections of wild-type and *Nde1*^{-/-} brains (at 8 weeks old) stained with H&E, which shows that the *Nde1*^{-/-} brain is smaller, with thinner cerebral cortex, but grossly normal.

(D) Sagittal sections that show the *Nde1*^{-/-} hippocampus is of normal size and structure, and the thinning of cerebral cortex is observed throughout the entire brain.

(E) Sagittal sections of *Nde1*^{+/-} and *Nde1*^{-/-} brain, which show an essentially normal cerebellum in the *Nde1*^{-/-} mice.

(F) Weight comparison and ratio of the anterior and posterior portions of the *Nde1*^{-/-} mutant brain (mean + SD). Homozygous *Nde1* mutant brains (n = 8) and the brains of their heterozygous counterparts (n = 8) are each separated into anterior and posterior part along the forebrain and midbrain junctions as indicated in the schematic diagram, and the weight of each part (“A” and “P”; mean + SD) and the ratio of anterior to posterior mass (R_{AP}; mean + SD) are presented. The figure shows that the weight of anterior forebrain in *Nde1*^{-/-} mutants is significantly reduced compared to that in the *Nde1*^{+/-} controls (p < 0.0001, by Student’s t test), whereas the posterior midbrain and cerebellum are only reduced slightly (p < 0.03, by Student’s t test).

(G) Coronal sections at three different levels (L1, L2, and L3, as shown in the diagram to the left) of the forebrain are compared between *Nde1* homozygous mutants (n = 6) and their heterozygous counterparts (n = 6). The area occupied by the six-layered neocortex on each section (highlighted in blue as dorsal brain) was measured and graphed as the ratio to the area of ventral brain structures, including the basal ganglia, the brain ventricles, the thalamus, the hippocampus, and the paleocortex (R_{D/V}; mean + SD). The figure shows that the neocortex in the *Nde1*^{-/-} mutant brain is reduced significantly in size relative to the basal brain structures at all three levels (p < 0.0001 in all three levels, by Student’s t test).

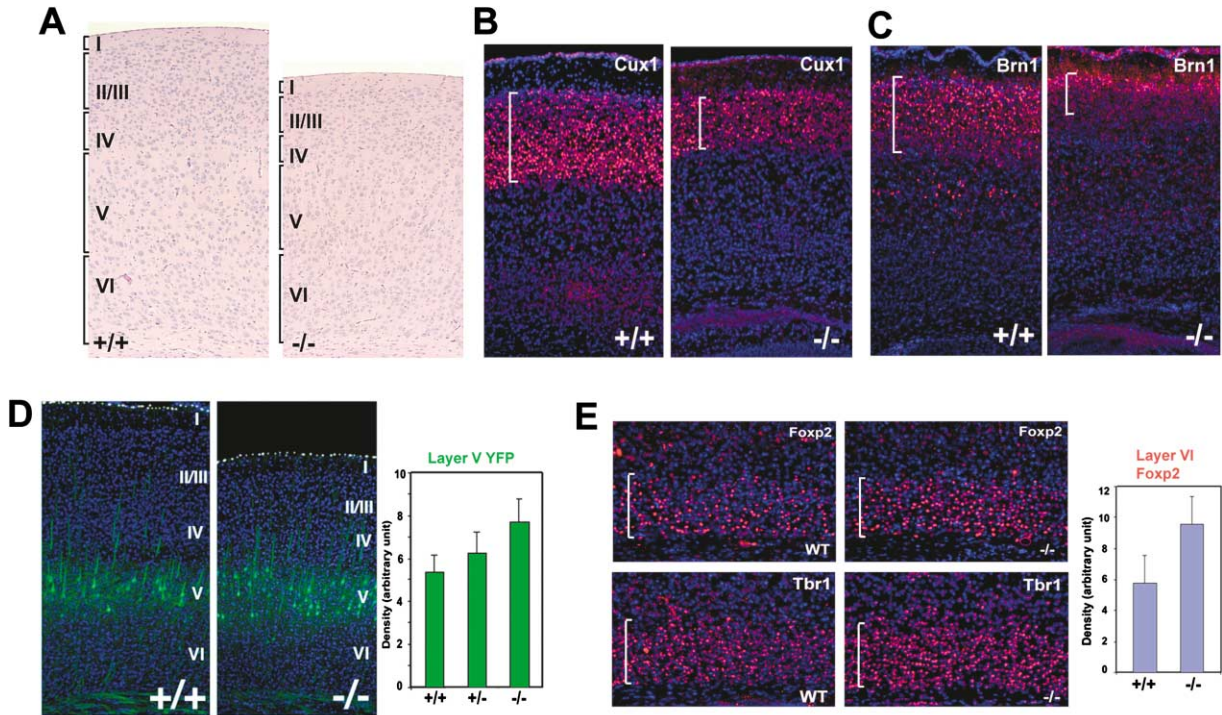


Figure 3. *Nde1* Homozygous Mutation Causes Thinning of the Superficial Cortical Layers

(A) Corresponding coronal sections of wild-type and *Nde1*^{-/-} neocortex stained with H&E, which shows the thinning of the cerebral cortex in *Nde1*^{-/-} mice and more dramatic reduction in cortical thickness and number of cortical neurons in cortical layers II/III to IV. Specific reduction of superficial cortical layers is also shown by decreased immunostaining of Cux1 and Brn1 at postnatal day 4, since Cux1 and Brn1 each mark a subset of neurons in cortical layers II to IV (B and C). The relative normal deeper cortical layer thickness is demonstrated by immunostaining with Foxp2 and Tbr1 antibodies at P4—both are markers for cortical layer VI (E)—and by crossing the *Nde1* mutation into a thy1-YFP transgenic line in which YFP is expressed predominantly in a subset of layer V neurons in the neocortex (D). All immunostaining signals were detected using Cy3-conjugated fluorescent secondary antibody shown in red, and sections were counterstained with Hoechst 33342 fluorescent dye in blue. The dotted lines indicate the position of cortical pial surface. The densities of YFP-positive neurons in layer V and Foxp2-positive neurons in layer VI are also presented (mean + SD). Compared with both wild-type and *Nde1* heterozygous, *Nde1* homozygous brain showed significant increase in YFP neuronal density ($p < 0.0001$ opposed to wild-type; $p < 0.002$ opposed to *Nde1*^{+/-}, by Student's *t* test). Similarly, the density of Foxp2-positive neurons in the *Nde1*^{-/-} cortex were significantly increased compared to the wild-type control ($p < 0.0001$, by Student's *t* test).

sistently thinner, with fewer cortical neurons than wild-type or *Nde1*^{+/-} littermates (Figures 2C and 2D). Moreover, the thinning of the cerebral cortex in *Nde1*^{-/-} mice was much more pronounced in superficial cortical layers, which are formed near the end of neurogenesis (Caviness et al., 1995; Rakic, 1978; Rakic and Caviness, 1995), whereas the earlier-born, deeper cortical layers were of normal to very slightly reduced thickness (Figure 3A). The upper border of the large pyramidal neurons that constitute layer V ends at about the same distance from the ventricular surface in the *Nde1*^{-/-} cortex as in control cortices, suggesting that the thicknesses of layer V and of layer VI beneath it are not significantly reduced. In contrast, layers II/III and IV are much thinner in the *Nde1*^{-/-} cortex (Figure 3A), while the marginal zone (layer I) is also of normal thickness.

The reduction of the superficial cortical layers was confirmed by immunostaining at postnatal day 4 with antisera to Cux1, which labels pyramidal cells in layers II through IV (Nieto et al., 2004), or to Brn1, which labels a subset of neurons in cortical layers II through IV (McEvilly et al., 2002) (Figures 3B and 3C). Moreover, the reduced Brn1-positive neural population displayed a

somewhat disordered distribution in *Nde1*^{-/-} mice, suggesting that a lamination defect was associated with *Nde1* mutation in upper layer neurons. The relatively normal thickness of deeper cortical layers at P4 was demonstrated by immunostaining with Foxp2 and Tbr1, which are markers for cortical layer VI (Ferland et al., 2003; Hevner et al., 2001), and by crossing the *Nde1* mutant allele into a thy1-YFP transgenic line (Feng et al., 2000a) in which YFP is expressed predominantly in a subset of layer V neurons in the neocortex (Figures 3D and 3E). Interestingly, although the thickness of layers V and VI appeared to be normal in the *Nde1*^{-/-} mice, we observed moderate but consistent increases in the density of YFP, Foxp2, and Tbr1 neurons in the mutant (Figures 3D and 3E), suggesting a cell fate alteration with increased proportions of specific deep layer neurons. We also examined neocortical interneurons that originated from the subcortical telencephalon by immunostaining with antibodies to calbindin and parvalbumin at various postnatal stages but did not find significant change in the density and distribution of these neurons (data not shown). Moreover, immunohistochemistry analysis with GFAP antibody did not show abnormal

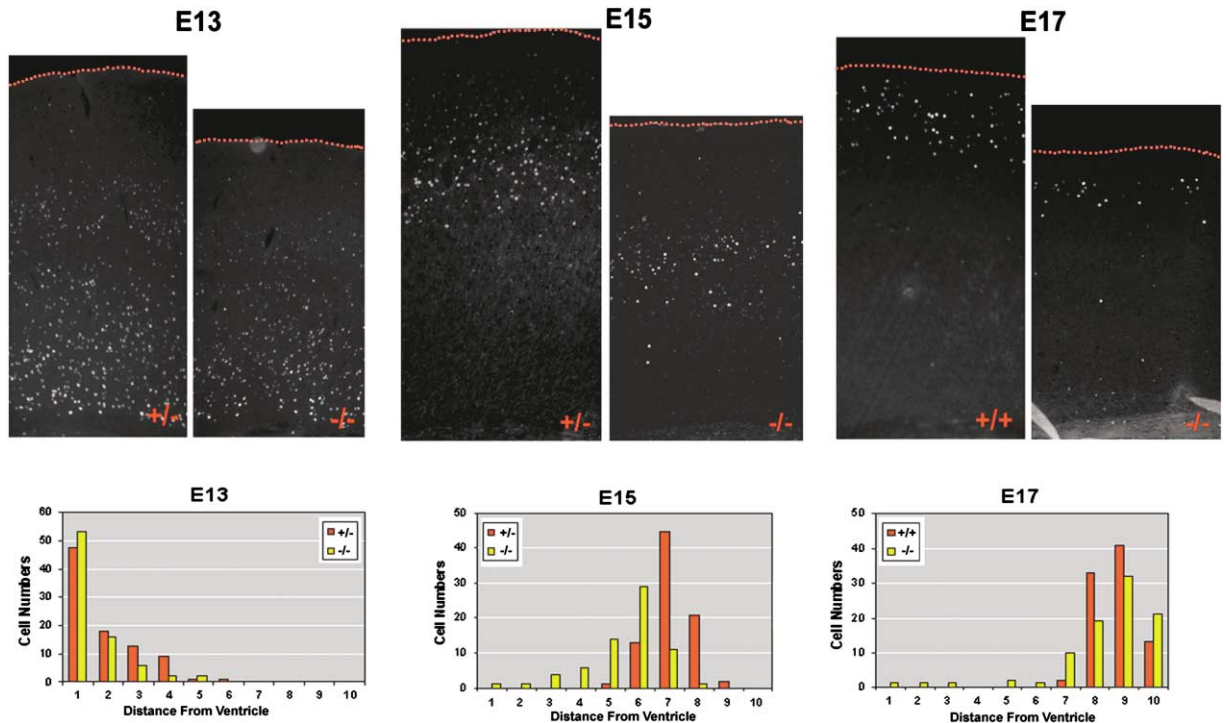


Figure 4. BrdU Birthdating Study Reveals Neuronal Migration Defect in *Nde1* Homozygous Mutants

Pregnant mice were injected intraperitoneally with BrdU at 50 $\mu\text{g/g}$ of body weight at E13, E15, and E17, respectively. The animals were analyzed 8–12 weeks postnatally. BrdU-positive neurons in the cerebral cortex were detected by immunostaining with a rat monoclonal antibody to BrdU (Harlan-Sera Lab). The density and distribution of BrdU-positive neurons from *Nde1* homozygous mutants and their wild-type or heterozygous littermates were analyzed. The cerebral cortex from both *Nde1*^{-/-} and control brain sections were each divided into ten equal layers, and the number of BrdU-stained neurons in each layer was plotted to represent the relative distance of neuronal migration from the ventricular surface. Two to four brains from *Nde1*^{-/-} mutant mice and their heterozygous or wild-type littermates were analyzed at each time point. Three pairs of representative sections of *Nde1*^{-/-} and control brains were shown. The dotted lines indicate the position of cortical pial surface.

gliogenesis in the *Nde1*^{-/-} brain (data not shown). Together, our data suggested that *Nde1* homozygous mutations had a specific impact on cortical neurons that arise from the cortical ventricular zone and reach the cortex through radial migration; the mutation produced a severe reduction in later-born superficial cortical neurons and a moderate increase in earlier-born deeper layer neurons.

Dual Defects of Neuronal Migration and Neurogenesis in *Nde1*^{-/-} Brain

BrdU birthdating was performed to examine whether the abnormalities in cortical layering reflected impaired neurogenesis, abnormal neuronal migration, or both. *Nde1* mutants were labeled by the thymidine analog 5-bromo-2'-deoxyuridine (BrdU), which is incorporated into the DNA of dividing progenitor cells and serves as a permanent marker if progenitors are labeled during the last mitotic cell cycle. When analyzed in adulthood, neurons labeled at E13 in the *Nde1*^{-/-} cortex showed a predominant deeper layer distribution indistinguishable from that in the wild-type and heterozygous littermate control cortex. However, fewer BrdU-positive neurons were observed in the adult *Nde1*^{-/-} brain when BrdU was administered at later stages of neurogenesis (E15 and E17). Moreover, neurons labeled at E15 and E17

showed a reduced distance of migration as well as a more scattered distribution in *Nde1*^{-/-} mutants relative to the wild-type or heterozygous controls (Figure 4). While these data, along with the *Bmn1* immunostaining, suggested that *Nde1* deficiency resulted in a neuronal migration defect, no gross defect of cortical layering or accumulation of later-born neurons in the deeper cortical layers and the white matter was observed. However, the consistent decrease in the overall number of neurons labeled by BrdU at E15 to E17 (Figure 4) suggested that *Nde1* deficiency induced proliferation defects in cortical progenitor cells.

Progressive Decrease in Cortical Progenitor Cells Caused by *Nde1* Deficiency

The defects in cortical progenitor proliferation in the *Nde1* homozygous mutants were further demonstrated by the progressive decrease in number of progenitor cells over the course of corticogenesis as shown by BrdU pulse labeling. When the embryonic brains were examined 30 min after BrdU administration, approximately equal numbers of BrdU-labeled progenitors were observed in *Nde1*^{+/-} and *Nde1*^{-/-} cortices at E12.5, while fewer BrdU-labeled cells were seen in *Nde1*^{-/-} cortex at E15. The difference in BrdU-labeled cells became even more pronounced at E17, when very few BrdU-

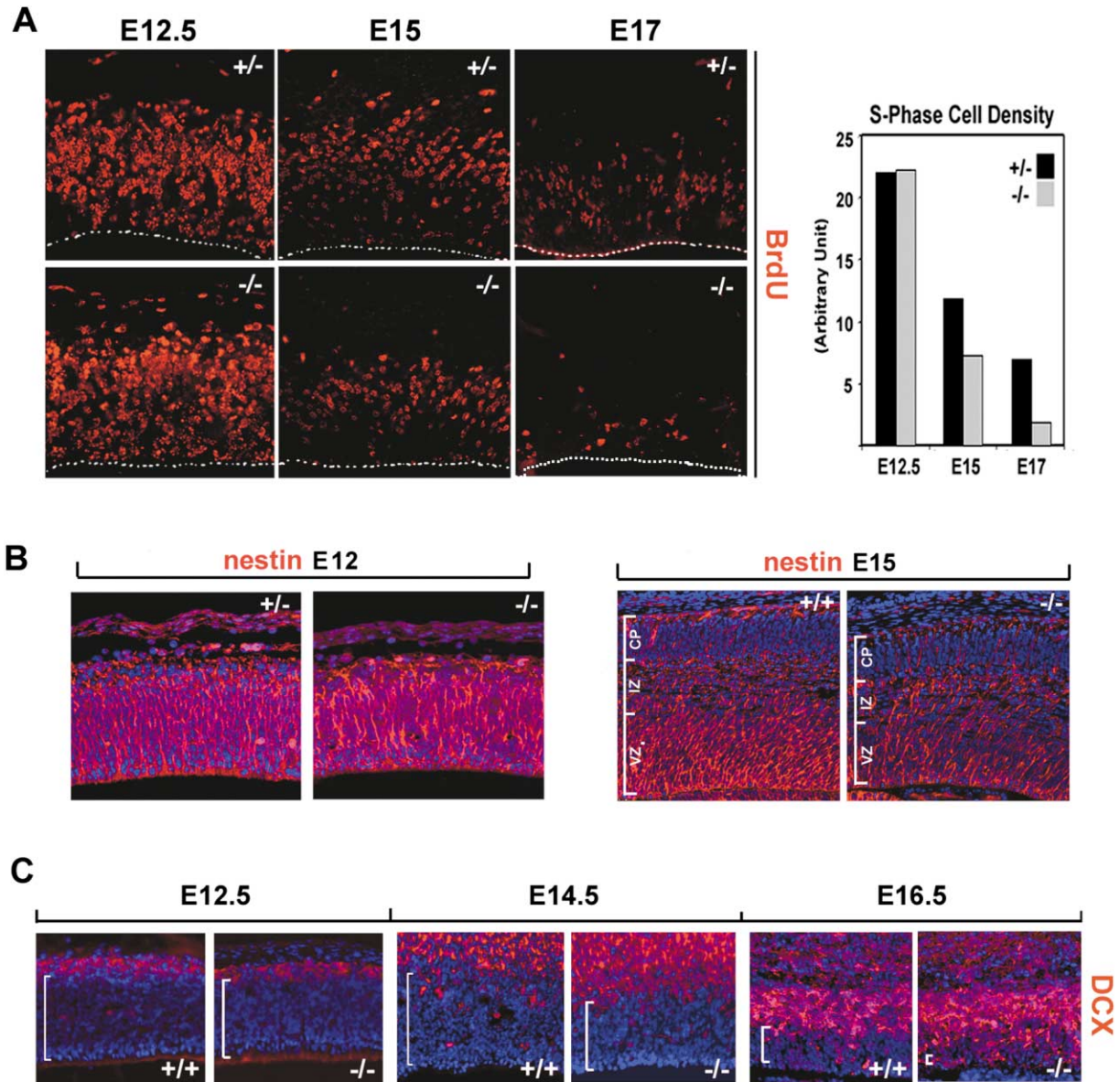


Figure 5. *Nde1* Deficiency Leads to Progressive Depletion of Cortical Progenitor Pool

(A) Analysis of S phase progenitor cells by BrdU pulse labeling of *Nde1*^{+/-} and *Nde1*^{-/-} embryos at E12.5, E15, and E17. BrdU was injected to pregnant females intraperitoneally at 50 μg/g of body weight. Embryos were fixed 30 min after the BrdU labeling and analyzed for BrdU-positive S phase cortical progenitors by staining the brain sections with monoclonal anti-BrdU antibody. Dotted lines indicate the position of cortical ventricular surface. The figure indicates a progressive reduction of S phase progenitor cells in the *Nde1*^{-/-} cortex relative to the *Nde1*^{+/-} control. In contrast to the normal number of S phase cells at E12.5, striking reduction in S phase progenitors associated with *Nde1* deletion was seen at E17, in which very few BrdU-positive cells were observed. The figure shown was representative of three repeated experiments. The relative densities of BrdU-labeled cells at E12.5, E15, and E17 in the figure are also presented.

(B) Nestin immunostaining (in red) of the cortex of *Nde1*^{-/-} embryos and their wild-type or heterozygous littermate controls at E12 and E15, which shows that the number of nestin-positive neuronal and radial glial progenitor cells appears to be normal at E12 but is significantly reduced in the *Nde1*^{-/-} cortex at E15. Brain sections were counterstained with Hoechst 33342 fluorescent dye in blue and shown as merged images.

(C) Brain sections from *Nde1*^{-/-} and their wild-type littermates were stained with antibody to Dcx (in red), which specifically expresses in newly differentiated postmitotic neurons. The sections were also counterstained with Hoechst 33342 fluorescent dye in blue. From E12.5 to E16.5, the size of cortical ventricular zone as presented by Dcx-devoid region is gradually reduced in the *Nde1* homozygous mutants.

positive cells were observed in the *Nde1*^{-/-} cortex (Figure 5A).

The progressive decrease in BrdU-positive progenitors was also in line with the progressively decreased nestin immunoreactivity in *Nde1*^{-/-} mice from E12 to E15 (Figure 5B), suggesting that the mutant mice either

failed to produce or had a net loss of progenitor cells during the course of corticogenesis. As a result, thinning of the cortical ventricular zone at mid to late stages of corticogenesis was observed by Dcx immunoreactivity, which showed that the ventricular zone, as represented by the Dcx-negative region, was significantly smaller in

the *Nde1*^{-/-} mutants than in wild-type controls at E14.5 and E16.5 (Figure 5C). Together, these data suggested that the loss of *Nde1* produced a progressive depletion of the progenitor pool during later stages of corticogenesis and consequently led to the observed reduction in late-born upper layer cortical neurons.

While we observed a very subtle increase in TUNEL staining in the *Nde1*^{-/-} cortex at E15 and E17 (data not shown), the total number of apoptotic cells in both control and the mutant brain remained very low, with typically one to three TUNEL-positive cells observed on each brain section. Such a low incidence seems insufficient to cause major changes in the progenitor pool and suggests that the increased apoptosis was not the primary cause of the neural progenitor reduction that we observed.

Mitotic Defects Are Responsible for the Reduction of Cortical Progenitor Pool

The *Nde1*^{-/-} mutant was further examined to understand the mechanism underlying the cortical progenitor pool reduction. We first observed that the loss of *Nde1* is associated with the accumulation of abnormal mitotic cells in the cortical ventricular zone. At E15, an approximately 1.8-fold increase in mitotic (metaphase and anaphase) cells was observed along the ventricular surface in the *Nde1*^{-/-} cortex compared to the *Nde1*^{+/-} control (Figure 6A), labeled either by Syto11 or using the mitotic marker phospho-Histone H3 (Figure 6C). The progressive reduction of progenitor cells, coupled with the accumulation of mitotic cells, strongly suggests a metaphase and/or an anaphase delay/arrest of neural progenitors in the *Nde1*^{-/-} brain.

The embryonic *Nde1*^{-/-} cortex also showed defects in the mitotic orientation of neural progenitor cells. While the majority of anaphase cells in normal E15 cortices displayed mitotic cleavage planes perpendicular to the ventricular surface (vertical cleavage), *Nde1*^{-/-} brains showed increased progenitors with mitotic cleavages parallel to the ventricular surface (horizontal cleavage) (Figure 6B). Vertically orientated cleavage planes are more commonly associated with “symmetrical” cell divisions, in which one progenitor generates two proliferative daughter cells, whereas horizontal cleavage planes often yield asymmetrical cell fates, with one proliferative daughter cell and a postmitotic neuron (Chenn and McConnell, 1995; Haydar et al., 2003; Noctor et al., 2004). Hence, the shift toward horizontal mitotic cleavages in *Nde1*^{-/-} brain correlates well with a change in cell fate that depletes the progenitor pool by increasing the proportion of cell divisions that generate postmitotic neuronal progeny and also suggests that the cell fate alteration that leads to increases in deeper layer neuronal populations (Figures 3D and 3E) might also be a reflection of the increased asymmetrical cell division in the *Nde1*^{-/-} progenitors.

The altered mitotic pattern in *Nde1*^{-/-} brains was further revealed by phospho-Histone H3 immunoreactivity, which showed the disordered localization of mitotic chromosomes associated with *Nde1* deficiency. Whereas most mitotic chromosomes are normally localized along the ventricular lumen, many *Nde1*^{-/-} mitotic chromosomes were found in the region above the ventricular

surface at both E13.5 and E15 (Figure 6C, green arrows). In neural epithelial cells, the position of the nucleus is known to correlate with the phase of the cell cycle, with nuclei of mitotic cells normally descending to the apical ventricular surface by interkinetic nuclear migration (Takahashi et al., 1996). The ectopic phospho-Histone H3 staining in *Nde1*^{-/-} mice thus reflects a partial dissociation of nuclear positioning from the cell cycle. As the position and the alignment of mitotic chromosomes are controlled by the mitotic spindle apparatus, the mispositioning of the mitotic chromosomes reflected abnormal assembly and structure of the mitotic spindle. Such a failure in mitotic spindle function might lead to the discoordination of the phase of cell cycle and mitotic chromosome segregation in the *Nde1*^{-/-} progenitor cells and produce mitotic abnormalities of the *Nde1*^{-/-} cortical progenitors.

Alteration of Neuronal Cell Fate by Mitotic Defects

While *Nde1* deficiency results in mitotic arrest/delay in cortical progenitor cells, it does not appear to completely block the mitosis of these cells by resulting in cell death. On the other hand, our observation of alteration in mitotic orientation toward vertical cleavage planes (potentially asymmetrical cell division), along with increased layer V and VI neuronal markers, suggested that mitotically arrested *Nde1*^{-/-} progenitor cells might be more likely to adopt a neuronal fate by exiting the cell cycle. We thus examined the possibility that reduced progenitor cells in the *Nde1*^{-/-} mice reflects a shift toward neuronal cell fate by examining the fraction of progenitor cells that exit the mitotic cell cycle during midneurogenesis (Takahashi et al., 1995). Mouse embryos were pulse labeled by BrdU injection into pregnant females at E14.5 and analyzed at E15.5 by double staining with BrdU and Ki67 antibodies (Chenn and Walsh, 2002). Since anti-Ki67 labels a nuclear transcription factor expressed from S phase through M phase, BrdU and Ki67 double-positive cells represent progenitors labeled at E14.5 that remain in the cell cycle, whereas BrdU-positive but Ki67-negative cells represent progenitors labeled at E14.5 that have exited the cell cycle at E15.5. We found that the fraction of BrdU-positive and Ki67-negative cells is 1.4-fold higher in the *Nde1*^{-/-} mice in comparison with that in the *Nde1*^{+/-} mice (Figure 6D), suggesting that more progenitor cells in the *Nde1* homozygous mutant adopt a postmitotic fate between E14.5 and E15.5. Since cortical neurogenesis at this stage produces neurons that comprise predominantly the deeper cortical layers, this result is consistent with the observation of denser cortical layer V and VI neurons in the *Nde1*^{-/-} mice (Figures 3D and 3E). In fact, the increase in the number of the earlier-born cortical layer neurons could be observed as early as E16.5, as indicated by elevated immunoreactivity of both *DCX* and *Tbr1* (Figures 6E and 6F), because both mark newly generated postmitotic cortical neurons at this stage. Together, these data further suggested that shifts toward neuronal fate may at least partially account for the progressive reduction of neural progenitors, leading to fewer late-born cortical neurons in the mutant mice. Thus, the small cerebral cortex phenotype seen in *Nde1*^{-/-} mice appears to be caused by mitotic spindle

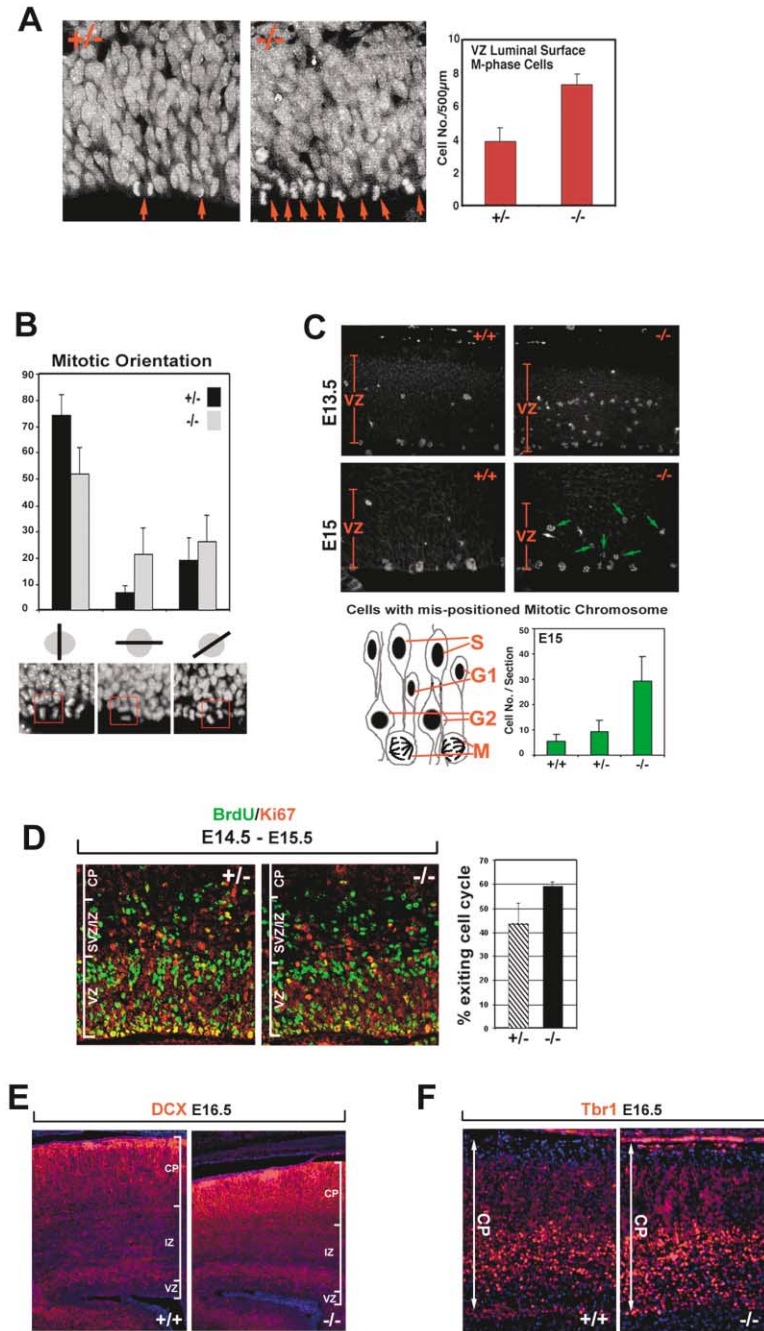


Figure 6. Mitotic Defects and Alteration of Neuronal Cell Fate in *Nde1* Homozygous Mutant Brain

(A) Accumulation of mitotic cells in the *Nde1*^{-/-} cortex. Confocal images of cortical ventricular zone stained with Syto11 show increased number of cells with condensed mitotic chromosomes (indicated by red arrows), suggesting mitotic arrest in *Nde1*^{-/-} brain at E15. Average numbers (mean + SD) of mitotic cells per 500 μm of ventricular lumen surface from coronal sections of three pairs of littermates are presented.

(B) Abnormal mitotic orientation of *Nde1*^{-/-} cortical progenitors at E15. Anaphase progenitor cells were classified into three groups according to the angle of mitotic cleavage plane to the ventricular surface (vertical, 75°–90°; horizontal, 0°–25°; and diagonal, 25°–75°). Percentage of each class of mitotic cleavage orientation from four pairs of *Nde1*^{+/-} and *Nde1*^{-/-} embryos at E15 were summarized (mean + SD). The figure indicates a dramatic reduction in symmetrical cell division with vertical cleavage planes ($p < 0.001$, by Student's *t* test) and corresponding increase in asymmetrical cell division in the *Nde1*^{-/-} neural progenitors ($p < 0.02$, by Student's *t* test). (C) Mispositioning of mitotic chromosomes in *Nde1*^{-/-} cortical progenitors. Immunostaining with the mitotic marker, the phospho-histone H3 antibody, indicates increases in number of mitotic progenitors with mispositioned chromosomes (pointed by green arrows) in the ventricular zone of E13.5 and E15 *Nde1*^{-/-} embryos. Average numbers of mispositioned M phase cells from three groups of E15 littermates (mean + SD) were presented with a diagram of normal nucleus positions in cortical neural progenitors in correlation to G1, S, G2, and M phases of the cell cycle.

(D) Cell cycle exit profiles of *Nde1*^{+/-} and *Nde1*^{-/-} mice. Embryos in pregnant *Nde1*^{+/-} females received a single dose of BrdU at E14.5 and were analyzed at E15.5. Brain sections were stained with antibodies to BrdU (in green) and to Ki67 (in red). Cells that exit the cell cycle are counted as those that are positive for BrdU but negative for Ki67 and are presented as the percentage of total BrdU-positive cells. An approximately 1.4-fold increase in cell cycle exit was observed in the *Nde1*^{-/-} cortex compared to the *Nde1*^{+/-} cortex ($p = 0.013$). The figure shows a representative of four experiments with three pairs of mutant and control littermates.

(E) Dcx staining of the E16.5 cerebral cortex,

which showed that the *Nde1*^{-/-} cortex had higher density of cortical plate neurons and suggested that a precocious neurogenesis is associated with the *Nde1* deficiency.

(F) Similarly, the density of Tbr1-positive neurons that comprise the deeper layers of the cortical plate also showed moderate elevation in the *Nde1*^{-/-} brain, suggesting a shift of cell fate toward the generation of more neurons in the *Nde1*^{-/-} mice. CP, cortical plate; IZ, intermediate zone; VZ, ventricular zone; SVZ, subventricular zone.

defects that result in mitotic delay/arrest, shifted mitotic orientation, altered neuronal cell fate, and failure in neural progenitor pool expansion.

Nde1 Is Required for Mitotic Spindle Assembly and Function

To understand the molecular function of Nde1 in cortical progenitor cell division, we investigated the role of Nde1

in mitosis in cultured cells. While Nde1 immunoreactivity localized to the centrosome in interphase cells (Figure 7A, “G1”), it highlighted the spindle poles and partially overlapped the spindle microtubules in mitotic cells. Moreover, punctate staining that strongly resembles the kinetochores also appeared in the midzone along the aligned mitotic chromosomes and decorated the tips of mitotic spindles during metaphase (Figure 7, “M” and

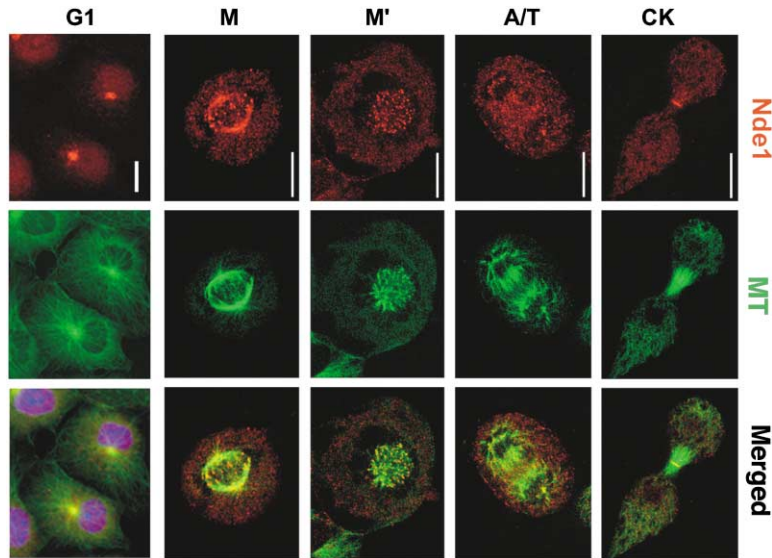


Figure 7. Nde1 Localizes to Important Sites for Mitotic Spindle Assembly and Chromosomal Segregation

The figure presents cell cycle-dependent localization of Nde1 in Cos7 cells. Indirect immunofluorescence staining of Nde1 (red) and microtubules (green) were visualized by laser scanning confocal microscopy. Merged images of Nde1 and microtubules are also shown. G1, interphase; M, metaphase; A/T, anaphase/telophase; CK, cytokinesis. Scale bar, 5 μ m. The figure indicates that Nde1 localizes to the mitotic spindle pole and the kinetochore during mitosis and to the midbody during cytokinesis.

“M”). While Nde1 immunoreactivity persisted at the spindle poles during anaphase and telophase (Figure 7, “A/T”), Nde1 also appeared in the cleavage furrow or the midbody during cytokinesis (Figure 7, “CK”). Together, these data indicated that Nde1 localizes to important sites for microtubule nucleation and bipolar spindle assembly and suggested that it may play a role in organizing mitotic microtubules.

We have previously shown that Nde1 appears to act as a scaffold interacting with multiple proteins and organizing them into functional complexes at the MTOC of interphase cells (Feng et al., 2000b). Moreover, Nde1 was also found to function as homodimers or oligomers. Yeast two-hybrid analysis suggested that the self-association of Nde1 is mediated through its N terminus (Supplemental Figure S1 at <http://www.neuron.org/cgi/content/full/44/2/279/DC1/>). Coimmunoprecipitation analysis of coexpressed GFP and myc-tagged Nde1 allowed us to map the Nde1 self-interaction domain to the N-terminal approximately 100 amino acids as represented by Nde1 truncation constructs N1 and N2 (Figures 8A and 8B). This self-association domain does not overlap with the binding domains for LIS1 and for other Nde1 binding partners (Feng et al., 2000b). Thus, in contrast to the specific blockage of Nde1-LIS1 interaction by overexpression of the LIS1 binding domain as previously shown (Feng et al., 2000b), overexpressing the truncated Nde1-N1 and -N2 constructs should specifically block any functions of Nde1 that require self-association but not affect Nde1-LIS1 and other Nde1 interactions.

Transient transfection of Nde1-N1 and -N2 into 293T cells induced severe mitotic arrest (Supplemental Figure S2 at <http://www.neuron.org/cgi/content/full/44/2/279/DC1/>) of cells with 4N DNA content as demonstrated by flow cytometry analysis (Figure 8C). Full-length Nde1, which expressed at a higher level than the Nde1-N1 and -N2 (Figure 8B), also enhanced the population of 4N DNA cells, but to a lesser extent than N1 and N2. These data suggested that blocking the dimerization/oligomerization of endogenous Nde1 by Nde1 N-ter-

минаl truncation constructs could efficiently induce mitotic arrest, whereas increased full-length recombinant Nde1 may also induce cell cycle arrest, perhaps by binding and sequestering the endogenous Nde1 dimer/oligomers. In contrast, no significant mitotic arrest was observed when LIS1 (which binds to Nde1 outside of the self-association domain), Nde1-LB (a Nde1 construct that binds LIS1) (Feng et al., 2000b), or Nde1-C (a C-terminal fragment of Nde1) were expressed under the same conditions, which further supports the notion that Nde1 dimerization/oligomerization through its N terminus is directly required for its scaffolding function in mitotic spindle assembly. While others have reported that expression of recombinant LIS1 also induces mitotic arrest (Faulkner et al., 2000), the difference might reflect the type of cell used and/or the level of recombinant LIS1 expression in various systems. However, the lack of effect of Nde1-LB under these conditions suggests that the effect of N-terminal Nde1 truncates is efficient and specific, and Nde1 is more directly required for mitotic progression relative to LIS1. As the first 100 amino acids of Nde1 are 90% homologous to the Nde1, Nde1-N1 may inhibit Nde1 as well, which might explain why the defects caused by Nde1-N1 are more severe than Nde1 homozygous mutations in mice.

A large fraction of M phase-arrested cells produced by Nde1-N1 overexpression showed severe mitotic spindle defects, including monopolar spindles, multipolar spindles, and mispositioned spindles (Figure 8D). Multipolar spindles were most common with partially or completely unattached and unaligned mitotic chromosomes. In many N1-expressing cells, the mitotic spindle was so poorly assembled that it was completely detached from the chromosomes (Figure 8D). While the centriolar protein centrin was localized to each pole of the multipolar spindle, additional centrin immunoreactivity, presumably representing extra centrioles, was also seen with no apparent association with spindle poles (Figure 8E, arrows). Since cells with odd numbers of centrioles (such as 3 and 5) were frequently observed by imaging through the entire Z series with confocal microscopy,

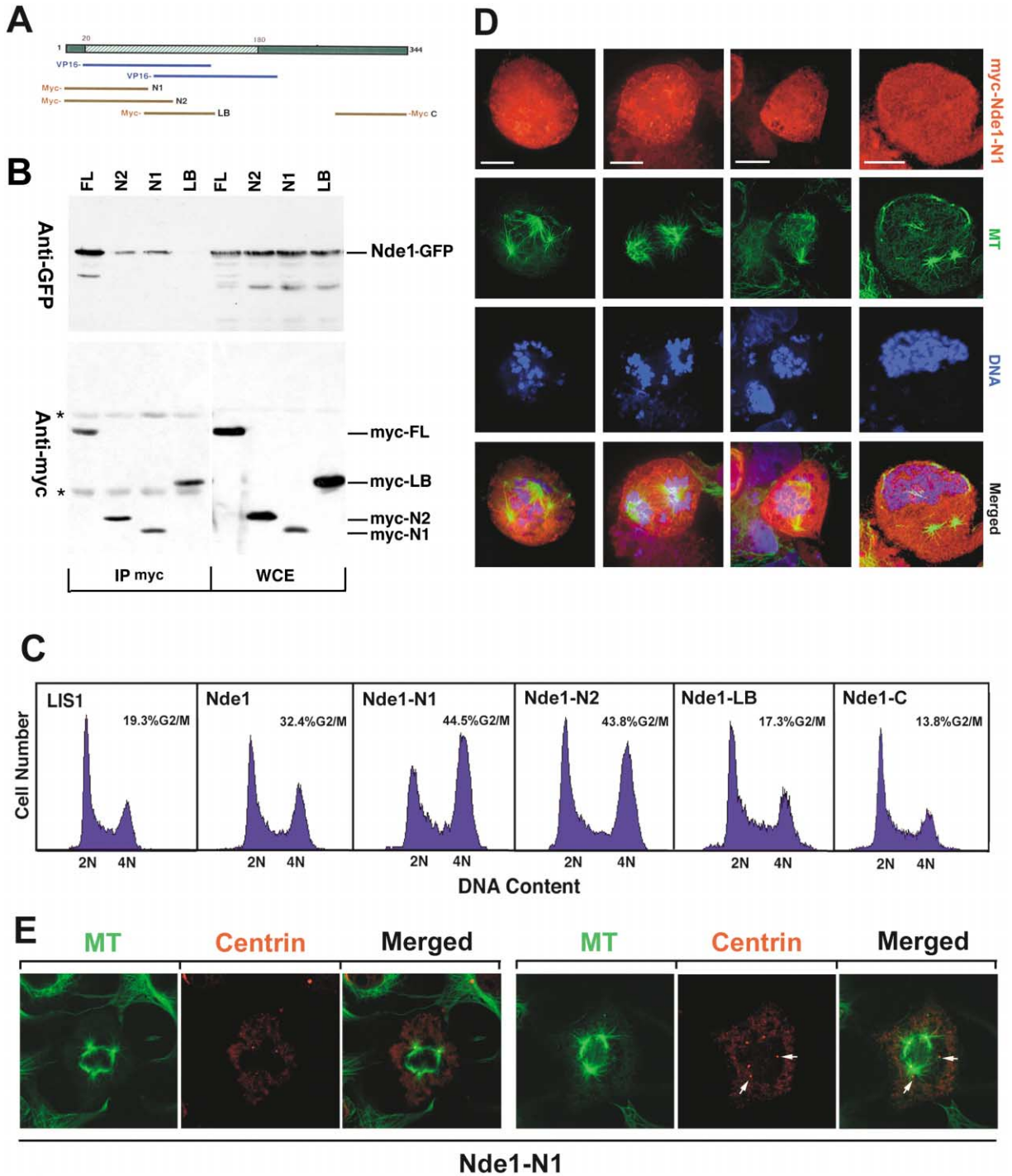


Figure 8. Nde1 Is Essential for Mitotic Spindle Assembly and Organization

(A) Structure diagram of Nde1 and Nde1 deletion constructs and mapping of Nde1 self-association domain through coimmunoprecipitation. The coiled-coil region from amino acid 20 to 180 of Nde1 is indicated by the hatched bar.

(B) Coimmunoprecipitation was performed to assess the interaction between myc- and GFP-tagged Nde1 expressed in 293T cells. Nde1 and its deletion constructs were tagged by the myc epitope and coexpressed with GFP-Nde1. Myc immunoprecipitation was performed from whole-cell protein extracts (WCE), and proteins precipitated by the myc antibody were analyzed on immunoblots with either anti-GFP or anti-myc antibodies. The asterisk denotes the heavy and light chains of IgG used in immunoprecipitation.

(C) Blocking self-association of Nde1 results in mitotic arrest. 293T cells were transfected with myc-tagged LIS1, Nde1, and Nde1 deletion constructs. Cells were harvested 40 hr posttransfection, fixed with 70% cold ethanol, and stained with anti-myc monoclonal antibody 9E10 followed by FITC-conjugated secondary anti-mouse antibody to indicate cells that express myc-tagged proteins. Propidium iodide was used to stain the nuclear DNA for analyzing the DNA content of myc-positive cells by flow cytometry. Cell cycle profiles of myc-positive cells are shown.

(D) Blocking the oligomerization by the N terminus of Nde1 induces defects in mitotic spindle assembly. Cos7 cells transfected by myc-tagged

and because abnormal mitotic spindles could be seen as early as 24 hr after Nde1-N1 transfection, the multiple spindle poles and centrioles induced by Nde1-N1 clearly did not result from failure in mitosis or cytokinesis. Instead, these data suggested that blocking Nde1 self-association induced defective centrosomal duplication, and this defect was at least partially responsible for spindle misassembly. Moreover, expression of Nde1-N1 in interphase cells does not induce microtubule depolymerization (Supplemental Figure S3 at <http://www.neuron.org/cgi/content/full/44/2/279/DC1/>), so the effect of Nde1-N1 on mitotic spindles thus appears to be specifically due to blocking Nde1's self-association and function.

Discussion

In summary, the findings reported here demonstrate that *Nde1* is essential for normal progenitor cell proliferation in the cerebral cortex. By being essential for centrosomal duplication and mitotic spindle assembly, it is required for controlling the speed and mode of cortical progenitor cell mitosis. Homozygous mutation of *Nde1* in mouse results in severe mitotic arrest/delay, alteration of mitotic orientation, and mispositioning of mitotic chromosomes in cortical progenitor cells. These mitotic defects are associated with the failure in maintenance of progenitor cell population, alterations of neural cell fates, progressive depletion of cortical progenitors, impaired neuronal migration, and a greatly reduced cerebral cortex with abnormal cortical layering. Our results suggest that mitotic spindle regulation by *Nde1* is not only essential for the proliferation of cortical progenitors but also has a great impact on neuronal fate determination and neuronal migration.

Nde1 Is Specifically Essential for Cerebral Cortex Development in Mouse

The relative specific requirement for *Nde1* in the cerebral cortex relative to other brain structures is somewhat surprising. Whereas other parts of the brain are probably somewhat affected in the mutant mouse, the cerebral cortex is clearly the focus of the effect. This may to some extent reflect the expression patterns of *Nde1* and its paralog, *Ndel1*. In mammals, *Nde1* is closely related to another LIS1-interacting protein, *Ndel1*, which shares almost 90% amino acid sequence homology in the N-terminal coiled-coil domain and more than 70% sequence homology over the full-length protein (Feng et al., 2000b; Niethammer et al., 2000; Sasaki et al., 2000). *Nde1* and *Ndel1* are also similar in many other cellular and molecular features, such as their subcellular local-

ization and their binding to LIS1 and to dynein motors (Feng et al., 2000b; Sasaki et al., 2000). They both form dimers or oligomers through their similar N-terminal domain (Sasaki et al., 2000). Therefore, the two genes may be genetically redundant in tissues/cells where they are coexpressed.

Although *Nde1* is widely expressed in mammals, its peak expression was observed in the cortical ventricular zone neural progenitor cells. In situ hybridization analysis demonstrated that the expression of *Nde1* in brain was specifically detected in the telencephalon between E12 and E16, and the expression of *Nde1* in the telencephalon is predominately seen in the cortical ventricular zone (Feng et al., 2000b) (Supplemental Figure S4 at <http://www.neuron.org/cgi/content/full/44/2/279/DC1/>). By early postnatal ages, *Nde1* mRNA can only be detected in residual cortical progenitor cells but is almost completely absent in the rest of the cerebral cortex and other brain structures (Supplemental Figure S4). In contrast, embryonic expression of *Ndel1* in CNS is complementary to *Nde1* and is detected in most regions of brain including the cortical plate but is largely excluded from cortical progenitor cells (Supplemental Figure S4). As *Ndel1* expression in CNS remains high postnatally and into adulthood (Sasaki et al., 2000), it is most likely essential for postnatal neuronal differentiation in the cerebral cortex and for the development of other CNS structures. As the two paralogs show overlapping expression in many non-CNS tissues during embryonic development (Supplemental Figure S4), the simplest mechanism for the cerebral cortex-specific *Nde1* mutant phenotype might be its tightly regulated expression in the cerebral cortex progenitors during neurogenesis. Therefore, *Ndel1* expression in other regions might rescue *Nde1* loss of function.

Nde1 and Mitotic Spindle Regulation in the Cerebral Cortex

An interesting question to consider is whether the cortical-specific expression of *Nde1* in turn reflects a distinct aspect of mitotic spindle regulation in cortical neural progenitors as opposed to elsewhere. For example, the narrow window of neurogenesis (between E12 and E17 in mouse) in the cortical ventricular zone progenitors requires a precise timing of cell division (Caviness et al., 1995; Takahashi et al., 1995), and we observed significant increases in metaphase and anaphase cell populations in the ventricular zone of the *Nde1*^{-/-} cortex at E15 and a similar increase in cells with 4N DNA content by blocking *Nde1* function in vitro. These suggest that the arrested/delayed mitosis and lengthened cell cycle contributed largely to the neuronal reduction in the *Nde1*^{-/-}

Nde1 N1 were fixed and costained with anti-myc and anti-tubulin antibodies to visualize myc-positive cells (in red) and microtubule/mitotic spindles (in green). Nuclear DNA was stained with Topro 3 iodide (in blue). Images were taken with a spinning disk confocal microscope. Four different examples are presented that show that expression of Nde1-N1 results in disorganized mitotic spindles with poorly structured spindle poles and unaligned and unattached mitotic chromosomes. Merged green, red, and blue images are also shown. Scale bar, 5 μ m.

(E) Abnormal centrosome duplication is responsible for Nde1-N1-induced spindle assembly defects. The centrosomal numbers in Nde1-N1-overexpressing cells were revealed by staining with the centriolar protein centrin (monoclonal antibody 20H5) in red. Microtubules were stained by a rat monoclonal anti-tubulin antibody (MCA77) in green. Images were analyzed using a spinning disk confocal microscope. Multiple Z sections were taken to reveal all centrioles and spindle poles, and one representative section is shown for each cell. While centrin staining was observed on most poles of the multipolar spindle, additional centrin signals that do not associate with spindle poles were also seen, suggesting that centrosome duplication defects in these cells are responsible for the abnormal spindle assembly.

mutant brain. As the neuronal reduction in *Nde1*^{-/-} mice was primarily observed in those cells that are derived from the neocortical ventricular proliferative zone, the cerebral cortex-specific size reduction due to *Nde1* mutation might, to a certain extent, reflect a specific speed requirement of mitosis of the ventricular zone progenitor cells.

The division of cortical progenitors is also precisely regulated by unique processes such as interkinetic nuclear migration, in which proper positioning of the mitotic chromosomes by proper assembly of the mitotic spindle appears to be pivotal for mitotic progression. In contrast to the severe dislocation of the mitotic nuclei from the ventricular surface in the *Nde1*^{-/-} progenitor cells (Figure 6C), most of the S phase progenitor cells were normally located in the outer half of the ventricular zone in the *Nde1*^{-/-} brain (Figure 5A, E15). This suggests that the interkinetic nuclear migration in the *Nde1* mutants was generally normal in cell cycle phases other than M phase; the specific abnormality associated with mitotic nuclei suggests a specific defect in the mitotic microtubule organization. Thus, the misposition of mitotic nuclei in the *Nde1*^{-/-} brain is more likely a direct reflection of disorganized mitotic spindles and/or detached mitotic chromosomes. However, current analysis with fixed tissue samples does not allow us to observe the mitotic spindle directly.

Mitotic Spindle and Neuronal Cell Fate

Nde1 mutant mice show an association of abnormal mitotic spindle orientation and abnormal neuronal cell fate choice, suggesting, though not proving, a linkage between these two processes. Time-lapse imaging has revealed that symmetrical cell divisions result in two daughter progenitor cells, whereas asymmetrical cell divisions appear to produce an apical progenitor cell and a basal postmitotic neuron (Chenn and McConnell, 1995; Haydar et al., 2003). In developing *Drosophila* nervous system, asymmetrical localization of cell fate determinants such as PROSPERO, NUMB, and Lgl to the basal surface of neuroblasts is essential for production of distinct cell types (Doe and Spana, 1995; Hirata et al., 1995; Knoblich et al., 1995; Peng et al., 2000; Rhyu et al., 1994; Roegiers et al., 2001). As some of these fate determinants are also asymmetrically localized in mouse cerebral cortical progenitors and might be critical for asymmetrical cell fates, normal mitotic spindle orientation might be a shared molecular mechanism for generating normal cell fates in both vertebrates and invertebrates (Klezovitch et al., 2004; Shen et al., 2002; Zhong et al., 1996).

Recent studies in the *Drosophila* testis have specifically shown the essential role of spindle components not just for proliferation, but also for the normal generation of cell fates that rely on the asymmetrical inheritance of cell fate determining factors (Yamashita et al., 2003). Mutations in the *Drosophila* centrosomin gene, which encodes a widely expressed component of the mitotic spindle apparatus, produces alteration in the normal exquisitely controlled pattern of mitotic spindle orientation in the testis and consequently changes the inheritance of cell fate components that are normally expressed but abnormally inherited because of the alteration in

mitotic spindle orientation relative to this expression pattern (Yamashita et al., 2003).

Nde1 was previously shown to be a central scaffold of multiple centrosomal proteins in interphase cells (Feng et al., 2000b). Our study now shows that it also plays important roles in proper duplication of the centrosome and the assembly of bipolar spindles at the onset of mitosis. *Nde1* may perform similar functions to centrosomin in determining cell fates in ventricular zone progenitors by regulating centrosomal position as well as mitotic spindle orientation, so that proper mitotic division planes are coordinated with the polarized expression of cell fate determinants such as numb (Zhong et al., 1996) or β -catenin (Chenn and Walsh, 2002). In the *Nde1* mutant, altered spindle orientation is associated with precocious withdrawal of progenitor cells from the cell cycle and precocious formation of neurons as assayed by increased immunoreactivity to *Dcx*, *Foxp2*, and *Tbr1* and expression of YFP by layer V neurons. Although recent studies using the TIS21-GFP knockin mouse have suggested that oblique mitotic cleavage planes could also be compatible with symmetric distribution of the apical membrane and were not necessarily indicative of a cell biologically neurogenic division (Kosodo et al., 2004), it does not exclude the possibility that the apical membrane can be unequally distributed in abnormal mitotic cleavages caused by spindle defects. Thus, altered mitotic orientation associated with *Nde1* mutation is still likely to result in unequal separation of cell fate determinants. The cortical-specific defects of *Nde1*^{-/-} mice may reflect not only abnormalities in progenitor cell division, but also alteration in neuronal fate. While failure in progenitor pool expansion would result in reduced production of neurons throughout the entire course of corticogenesis, increased asymmetric mitoses might produce neurons at the expense of daughter progenitor cells during early corticogenesis, resulting in the seemingly normal thickness of deeper cortical layers as we observed. Therefore, *Nde1* is an ideal candidate for connecting spindle orientation to cell fate in cerebral cortical progenitors.

Nde1 and *Lis1*

The phenotype of *Nde1*^{-/-} mice closely resembles defects produced by *Lis1* mutations in mouse in affecting both neurogenesis and neuronal migration (Gambello et al., 2003; Hirotsune et al., 1998). Although homozygous *Lis1* knockout mice are peri-implantation lethal, compound heterozygous mice expressing 35% of the wild-type level of *Lis1* protein show severe defects in both neuronal migration and neurogenesis. Among various defects, a mitotic delay with increased numbers of M phase cells and with mispositioned mitotic nuclei was also found in the *Lis1* mutant embryos, which is similar to our observations in *Nde1* homozygous mutant mice (Gambello et al., 2003; Hirotsune et al., 1998). While LIS1 has been known to be required for cortical neuronal migration, the molecular function of LIS1 has been of intense interest and controversy (Faulkner et al., 2000; Hattori et al., 1995; Liu et al., 2000; Niethammer et al., 2000; Reiner et al., 1993; Sapir et al., 1997). In addition to cell migration, LIS1 has also been implicated in cell division through the observation that *Lis1* null cells in

Drosophila show proliferation defects and that decreased LIS1 activity induced mitotic arrest in mammalian cell culture (Faulkner et al., 2000; Liu et al., 2000). Therefore, it is highly likely that LIS1 and Nde1 are in the same molecular and genetic pathway in regulating progenitor cell mitosis.

On the other hand, the restriction of *Nde1* loss-of-function phenotype to the six-layered neocortex and specifically to neurons originating from the cortical ventricular precursors correlates very well with the observation that haploinsufficiency of *LIS1* in humans mostly presents as a cerebral cortex-specific defect with little impact on other brain structures such as the cerebellum and basal ganglia (Barkovich et al., 1991; Dobyns et al., 1993). This suggests that cortical progenitor cell proliferation defects may also underlie the pathogenesis of lissencephaly in humans. Since neural progenitor cell division occurs prior to and is tightly coupled to neuronal migration, the defects in the mode and duration of progenitor proliferation may have a strong impact on subsequent neuronal migration processes. Moreover, we observed a significant reduction of nestin-positive cells in the cortex of *Nde1*^{-/-} mice by E15, which suggested that the mutant *Nde1* mice may also have defective radial glia processes due to mitotic arrest of both neural and radial glial progenitors (Noctor et al., 2002). The potential radial glia defect could also contribute to the migration difficulties of neurons in these mice. As both *Nde1* homozygous and *Lis1* heterozygous mice show modest neuronal migration abnormalities, further study of the correlation between cortical progenitor mitosis and cortical neuronal migration with genetic models of *Nde1* and *Lis1* double mutations would allow a better understanding of the mechanism of both molecules in corticogenesis and the pathological basis of lissencephaly.

Nde1 and Other Microcephaly Genes

It is also interesting that the microcephaly of *Nde1* mutant mice resembles what is observed in abnormal spindle protein microcephaly (*ASPM*)-associated microcephaly in human (Bond et al., 2002), and the expression patterns of *ASPM* and *Nde1* are very similar. Like *Nde1*, the *Drosophila* homolog of *ASPM*, *Asp*, is functionally important for microtubule organization at the spindle pole, and mutations of *Asp* in *Drosophila* result in aberrant mitotic spindle formation and metaphase arrest (do Carmo Avides and Glover, 1999). Thus, the molecular mechanism of *Nde1* and *ASPM* in cortical progenitor cell division could be quite similar. Moreover, the preferential loss of neurons in layers II to IV in the *Nde1* mutant matches the most common pathological finding in human genetic forms of microcephaly (Mochida and Walsh, 2001), in which the cerebral cortex becomes reduced in size. Therefore, *Nde1* mutant mouse may also represent an important animal model for these disorders. It would be interesting to further explore whether *Nde1*, *ASPM*, and other microcephaly genes act on a common molecular pathway that is critical for determining the size of the mammalian cerebral cortex developmentally, as well as whether they are targets for the evolutionary forces that have increased cerebral cortical size so dramatically between rodents and humans.

Experimental Procedures

DNA Constructs

Myc-Nde1, myc-LB (referred to as myc-DN previously), myc-LIS1, GFP-Nde1, and the VP16-Nde1 constructs were described previously (Feng et al., 2000b). The N-terminal and C-terminal Nde1 deletion constructs N1, N2, and C were generated by PCR amplification of the Nde1 cDNA encoding amino acids 1–93, 1–111, and 281–341, respectively, followed by subcloning the PCR products into pcDNA3 (Invitrogen).

Generation of Nde1 Mutant Mice

To generate targeted deletion of Nde1 protein, exon 2 of the mouse *Nde1* gene was flanked with loxP sites, so that deletion of the exon 2 by Cre-mediated recombination results in a nonsense mutation that truncates the Nde1 protein at amino acid 27. The targeting vector was introduced to mouse ES cells by conventional gene-targeting techniques. *Nde1*-targeted clones were further transfected with a Cre-recombinase expression plasmid, and the removal of neomycin and TK cassette alone or with exon2 of *Nde1* gene was selected with gancyclovir. Cre recombinant clones that were identified by Southern blotting were injected into C57BL/6 blastocysts and subsequently transmitted into the germline by breeding the male chimeric mice with the wild-type outbred Black Swiss females.

Histology and Quantitative Analysis

Mouse tissues were fixed by 4% paraformaldehyde followed by cryoprotection in 30% sucrose or embedded in paraffin. Cryostat sections were cut at 12–16 μ m, and paraffin blocks were sectioned at 5 μ m. Brain sections were stained with hematoxylin-eosin (H&E). Immunofluorescence was carried out by blocking in 5%–10% goat or donkey serum and 0.05% Triton X-100 in PBS for 1 hr, followed by incubation with primary antibody at 4°C overnight in the same solution. Sections were washed in PBS, followed by incubation with appropriate fluorescence-conjugated secondary antibodies for visualizing the immunosignals.

Quantitative measurement of cortical cell numbers was performed on photomicrographs of comparable coronal sections for each genotype using either Scion image 1.63 or ImageJ image processing and analysis software. The number of mice in each experiment was at least three per genotype. Data were presented as mean + SD. The statistical significance of differences between *Nde1*^{-/-} and control samples was assessed by one-way ANOVA with pairwise comparisons or by Student's t test.

BrdU Labeling and Analysis

Pregnant mice were injected intraperitoneally with BrdU at 50 μ g/g of body weight. The animals were either sacrificed 30 min after the injection for analysis of BrdU pulse-labeled S phase progenitor cells or in 24 hr for examination of cell cycle exits of the labeled progenitors. Alternatively, BrdU-labeled pregnant females were left to give birth, and their offspring were analyzed 8–12 weeks postnatally in the birthdating study. BrdU-positive neurons in the cerebral cortex were detected by immunostaining 2N HCl-treated brain sections with a rat monoclonal antibody to BrdU (Harlan-Sera Lab). The density and distribution of BrdU-positive neurons from *Nde1* homozygous mutants and their wild-type or heterozygous littermates were analyzed.

Cell Culture, Transfection, and Immunofluorescence Microscopy

Cos7 and 293T cells were grown in DMEM with 10% FBS, transfected, and analyzed as described (Feng et al., 2000b). Indirect immunofluorescence images were taken either with an Olympus AX70 fluorescence microscope, a BioRad Radiance 2000 confocal microscope, or a Nikon TE2000/PerkinElmer Ultraview spinning disk confocal microscope.

Coimmunoprecipitation and Immunoblotting

Nde1 and its deletion constructs were tagged by the myc epitope and cotransfected with GFP-Nde1 in 293 cells. Myc immunoprecipitation was performed from whole-cell protein extracts (WCE) 40 hr after transfection as described (Feng et al., 2000b); proteins precipi-

tated by anti-myc antibody were analyzed on immunoblots with either anti-GFP (Clontech) or anti-myc antibodies using enhanced chemiluminescence (ECL) detection (KPL).

Flow Cytometry Analysis

For analysis of cell DNA content, 293T cells were transfected with either GFP-tagged or myc-tagged expression construct of LIS1 or Nde1. Forty hours after transfection, cells were fixed with 70% cold ethanol at -20°C for more than 24 hr. Cells expressing GFP-tagged proteins were labeled with 50 $\mu\text{g/ml}$ propidium iodide and then subjected to flow cytometry analysis. For myc-tagged proteins, the cells were rehydrated in PBS after cold ethanol fixation, blocked in PBS plus 2% goat serum, and stained with 5 mg/ml 9E10 antibody followed by a FITC-conjugated goat anti-mouse secondary antibody. The cells were then postfixed for 1 hr with 1% formaldehyde in PBS and stained with 50 $\mu\text{g/ml}$ propidium iodide for flow cytometry analysis. The fluorescence of cells was measured and analyzed by a Becton-Dickinson FACScan flow cytometer.

Acknowledgments

We would like to thank members of the Walsh lab for stimulating discussions. Special gratitude goes to J. Corbo for constructing the backbone of the gene-targeting vector used in this study as well as his help in screening the mouse genomic library; Tam Thompson at the Center for Mental Retardation at the Children's Hospital of Boston (supported by NICHD P30HD18655) for assistance in generating *Nde1*-targeted mouse ES cells; and Dr. Arlene Sharp and Lina Du (Brigham and Women's Hospital) for mouse blastocyst injections. We are also grateful to Dr. Marc Kirschner (Harvard Medical School) for reading and providing helpful comments on an earlier version of the manuscript; to Drs. Paul Chang (Tim Mitchison lab, Harvard Medical School) and Robert Hevner (University of Washington) for sharing centrin and *Tbr1* antibodies. This work was supported by research grants from the NINDS to C.A.W. (P01 NS40043 and RO1 NS032457). C.A.W. is an investigator of the Howard Hughes Medical Institute. Y.F. is supported by an award from NIMH (K01MH065338) and a postdoctoral fellowship from the Charles A. King Trust.

Received: June 17, 2004

Revised: September 7, 2004

Accepted: September 16, 2004

Published: October 13, 2004

References

Barkovich, A.J., Koch, T.K., and Carrol, C.L. (1991). The spectrum of lissencephaly: report of ten patients analyzed by magnetic resonance imaging. *Ann. Neurol.* **30**, 139–146.

Barkovich, A.J., Kuzniecky, R.I., Dobyns, W.B., Jackson, G.D., Becker, L.E., and Evrard, P. (1996). A classification scheme for malformations of cortical development. *Neuropediatrics* **27**, 59–63.

Bond, J., Roberts, E., Mochida, G.H., Hampshire, D.J., Scott, S., Askham, J.M., Springell, K., Mahadevan, M., Crow, Y.J., Markham, A.F., et al. (2002). ASPM is a major determinant of cerebral cortical size. *Nat. Genet.* **32**, 316–320.

Caviness, V.S., Jr., Takahashi, T., and Nowakowski, R.S. (1995). Numbers, time and neocortical neurogenesis: a general developmental and evolutionary model. *Trends Neurosci.* **18**, 379–383.

Chenn, A., and McConnell, S.K. (1995). Cleavage orientation and the asymmetric inheritance of Notch1 immunoreactivity in mammalian neurogenesis. *Cell* **82**, 631–641.

Chenn, A., and Walsh, C.A. (2002). Regulation of cerebral cortical size by control of cell cycle exit in neural precursors. *Science* **297**, 365–369.

D'Arcangelo, G., Miao, G.G., Chen, S.C., Soares, H.D., Morgan, J.I., and Curran, T. (1995). A protein related to extracellular matrix proteins deleted in the mouse mutant reeler. *Nature* **374**, 719–723.

des Portes, V., Francis, F., Pinard, J.M., Desguerre, I., Moutard, M.L., Snoeck, I., Meiners, L.C., Capron, F., Cusmai, R., Ricci, S., et al. (1998). doublecortin is the major gene causing X-linked subcortical laminar heterotopia (SCLH). *Hum. Mol. Genet.* **7**, 1063–1070.

Dobyns, W.B., and Truwit, C.L. (1995). Lissencephaly and other malformations of cortical development: 1995 update. *Neuropediatrics* **26**, 132–147.

Dobyns, W.B., Reiner, O., Carrozzo, R., and Ledbetter, D.H. (1993). Lissencephaly. A human brain malformation associated with deletion of the LIS1 gene located at chromosome 17p13. *JAMA* **270**, 2838–2842.

do Carmo Avides, M., and Glover, D.M. (1999). Abnormal spindle protein, Asp, and the integrity of mitotic centrosomal microtubule organizing centers. *Science* **283**, 1733–1735.

Doe, C.Q., and Spana, E.P. (1995). A collection of cortical crescents: asymmetric protein localization in CNS precursor cells. *Neuron* **15**, 991–995.

Efimov, V.P., and Morris, N.R. (2000). The LIS1-related NUDF protein of *Aspergillus nidulans* interacts with the coiled-coil domain of the NUDE/RO11 protein. *J. Cell Biol.* **150**, 681–688.

Faulkner, N.E., Dujardin, D.L., Tai, C.Y., Vaughan, K.T., O'Connell, C.B., Wang, Y., and Vallee, R.B. (2000). A role for the lissencephaly gene LIS1 in mitosis and cytoplasmic dynein function. *Nat. Cell Biol.* **2**, 784–791.

Feng, G., Mellor, R.H., Bernstein, M., Keller-Peck, C., Nguyen, Q.T., Wallace, M., Nerbonne, J.M., Lichtman, J.W., and Sanes, J.R. (2000a). Imaging neuronal subsets in transgenic mice expressing multiple spectral variants of GFP. *Neuron* **28**, 41–51.

Feng, Y., Olson, E.C., Stukenberg, P.T., Flanagan, L.A., Kirschner, M.W., and Walsh, C.A. (2000b). LIS1 regulates CNS lamination by interacting with mNudE, a central component of the centrosome. *Neuron* **28**, 665–679.

Ferland, R.J., Cherry, T.J., Preware, P.O., Morrissey, E.E., and Walsh, C.A. (2003). Characterization of *Foxp2* and *Foxp1* mRNA and protein in the developing and mature brain. *J. Comp. Neurol.* **460**, 266–279.

Fox, J.W., Lamperti, E.D., Eksioğlu, Y.Z., Hong, S.E., Feng, Y., Graham, D.A., Scheffer, I.E., Dobyns, W.B., Hirsch, B.A., Radtke, R.A., et al. (1998). Mutations in filamin 1 prevent migration of cerebral cortical neurons in human periventricular heterotopia. *Neuron* **21**, 1315–1325.

Gambello, M.J., Darling, D.L., Yingling, J., Tanaka, T., Gleeson, J.G., and Wynshaw-Boris, A. (2003). Multiple dose-dependent effects of *Lis1* on cerebral cortical development. *J. Neurosci.* **23**, 1719–1729.

Gleeson, J.G., Allen, K.M., Fox, J.W., Lamperti, E.D., Berkovic, S., Scheffer, I., Cooper, E.C., Dobyns, W.B., Minnerath, S.R., Ross, M.E., and Walsh, C.A. (1998). Doublecortin, a brain-specific gene mutated in human X-linked lissencephaly and double cortex syndrome, encodes a putative signaling protein. *Cell* **92**, 63–72.

Hattori, M., Adachi, H., Aoki, J., Tsujimoto, M., Arai, H., and Inoue, K. (1995). Cloning and expression of a cDNA encoding the beta-subunit (30-kDa subunit) of bovine brain platelet-activating factor acetylhydrolase. *J. Biol. Chem.* **270**, 31345–31352.

Haydar, T.F., Ang, E., Jr., and Rakic, P. (2003). Mitotic spindle rotation and mode of cell division in the developing telencephalon. *Proc. Natl. Acad. Sci. USA* **100**, 2890–2895.

Hevner, R.F., Shi, L., Justice, N., Hsueh, Y., Sheng, M., Smiga, S., Bulfone, A., Goffinet, A.M., Campagnoni, A.T., and Rubenstein, J.L. (2001). *Tbr1* regulates differentiation of the preplate and layer 6. *Neuron* **29**, 353–366.

Hirata, J., Nakagoshi, H., Nabeshima, Y., and Matsuzaki, F. (1995). Asymmetric segregation of the homeodomain protein Prospero during *Drosophila* development. *Nature* **377**, 627–630.

Hirotsune, S., Fleck, M.W., Gambello, M.J., Bix, G.J., Chen, A., Clark, G.D., Ledbetter, D.H., McBain, C.J., and Wynshaw-Boris, A. (1998). Graded reduction of *Pafah1b1* (*Lis1*) activity results in neuronal migration defects and early embryonic lethality. *Nat. Genet.* **19**, 333–339.

Kato, M., and Dobyns, W.B. (2003). Lissencephaly and the molecular basis of neuronal migration. *Hum. Mol. Genet.* **12**, R89–R96.

Klezovitch, O., Fernandez, T.E., Tapscott, S.J., and Vasioukhin, V. (2004). Loss of cell polarity causes severe brain dysplasia in *Lgl1* knockout mice. *Genes Dev.* **18**, 559–571.

- Knoblich, J.A., Jan, L.Y., and Jan, Y.N. (1995). Asymmetric segregation of Numb and Prospero during cell division. *Nature* 377, 624–627.
- Kosodo, Y., Roper, K., Haubensak, W., Marzesco, A.M., Corbeil, D., and Huttner, W.B. (2004). Asymmetric distribution of the apical plasma membrane during neurogenic divisions of mammalian neuroepithelial cells. *EMBO J.* 23, 2314–2324.
- Liu, Z., Steward, R., and Luo, L. (2000). *Drosophila* Lis1 is required for neuroblast proliferation, dendritic elaboration and axonal transport. *Nat. Cell Biol.* 2, 776–783.
- McEvelly, R.J., de Diaz, M.O., Schonemann, M.D., Hooshmand, F., and Rosenfeld, M.G. (2002). Transcriptional regulation of cortical neuron migration by POU domain factors. *Science* 295, 1528–1532.
- Mochida, G.H., and Walsh, C.A. (2001). Molecular genetics of human microcephaly. *Curr. Opin. Neurol.* 14, 151–156.
- Niethammer, M., Smith, D.S., Ayala, R., Peng, J., Ko, J., Lee, M.S., Morabito, M., and Tsai, L.H. (2000). NUDEL is a novel Cdk5 substrate that associates with LIS1 and cytoplasmic dynein. *Neuron* 28, 697–711.
- Nieto, M., Monuki, E.S., Tang, H., Imitola, J., Haubst, N., Khoury, S.J., Cunningham, J., Gotz, M., and Walsh, C.A. (2004). Expression of Cux-1 and Cux-2 in the subventricular zone and upper layers II–IV of the cerebral cortex. *J. Comp. Neurol.*, in press.
- Noctor, S.C., Flint, A.C., Weissman, T.A., Wong, W.S., Clinton, B.K., and Kriegstein, A.R. (2002). Dividing precursor cells of the embryonic cortical ventricular zone have morphological and molecular characteristics of radial glia. *J. Neurosci.* 22, 3161–3173.
- Noctor, S.C., Martinez-Cerdeno, V., Ivic, L., and Kriegstein, A.R. (2004). Cortical neurons arise in symmetric and asymmetric division zones and migrate through specific phases. *Nat. Neurosci.* 7, 136–144.
- Olson, E.C., and Walsh, C.A. (2002). Smooth, rough and upside-down neocortical development. *Curr. Opin. Genet. Dev.* 12, 320–327.
- Peng, C.Y., Manning, L., Albertson, R., and Doe, C.Q. (2000). The tumour-suppressor genes *lgl* and *dlg* regulate basal protein targeting in *Drosophila* neuroblasts. *Nature* 408, 596–600.
- Pilz, D.T., Matsumoto, N., Minnerath, S., Mills, P., Gleeson, J.G., Allen, K.M., Walsh, C.A., Barkovich, A.J., Dobyns, W.B., Ledbetter, D.H., and Ross, M.E. (1998). LIS1 and XLIS (DCX) mutations cause most classical lissencephaly, but different patterns of malformation. *Hum. Mol. Genet.* 7, 2029–2037.
- Rakic, P. (1978). Neuronal migration and contact guidance in the primate telencephalon. *Postgrad. Med. J. Suppl.* 54, 25–40.
- Rakic, P. (1988a). Defects of neuronal migration and the pathogenesis of cortical malformations. *Prog. Brain Res.* 73, 15–37.
- Rakic, P. (1988b). Specification of cerebral cortical areas. *Science* 241, 170–176.
- Rakic, P. (1995). A small step for the cell, a giant leap for mankind: a hypothesis of neocortical expansion during evolution. *Trends Neurosci.* 18, 383–388.
- Rakic, P., and Caviness, V.S., Jr. (1995). Cortical development: view from neurological mutants two decades later. *Neuron* 14, 1101–1104.
- Reiner, O., Carrozzo, R., Shen, Y., Wehnert, M., Faustinella, F., Dobyns, W.B., Caskey, C.T., and Ledbetter, D.H. (1993). Isolation of a Miller-Dieker lissencephaly gene containing G protein beta-subunit-like repeats. *Nature* 364, 717–721.
- Rhyu, M.S., Jan, L.Y., and Jan, Y.N. (1994). Asymmetric distribution of numb protein during division of the sensory organ precursor cell confers distinct fates to daughter cells. *Cell* 76, 477–491.
- Roegiers, F., Younger-Shepherd, S., Jan, L.Y., and Jan, Y.N. (2001). Two types of asymmetric divisions in the *Drosophila* sensory organ precursor cell lineage. *Nat. Cell Biol.* 3, 58–67.
- Sapir, T., Elbaum, M., and Reiner, O. (1997). Reduction of microtubule catastrophe events by LIS1, platelet-activating factor acetylhydrolase subunit. *EMBO J.* 16, 6977–6984.
- Sasaki, S., Shionoya, A., Ishida, M., Gambello, M.J., Yingling, J., Wynshaw-Boris, A., and Hirotsune, S. (2000). A LIS1/NUDEL/cytoplasmic dynein heavy chain complex in the developing and adult nervous system. *Neuron* 28, 681–696.
- Shen, Q., Zhong, W., Jan, Y.N., and Temple, S. (2002). Asymmetric Numb distribution is critical for asymmetric cell division of mouse cerebral cortical stem cells and neuroblasts. *Development* 129, 4843–4853.
- Smith, D.S., Niethammer, M., Ayala, R., Zhou, Y., Gambello, M.J., Wynshaw-Boris, A., and Tsai, L.H. (2000). Regulation of cytoplasmic dynein behaviour and microtubule organization by mammalian Lis1. *Nat. Cell Biol.* 2, 767–775.
- Sweeney, K.J., Prokscha, A., and Eichele, G. (2001). NudE-L, a novel Lis1-interacting protein, belongs to a family of vertebrate coiled-coil proteins. *Mech. Dev.* 101, 21–33.
- Takahashi, T., Nowakowski, R.S., and Caviness, V.S., Jr. (1995). The cell cycle of the pseudostratified ventricular epithelium of the embryonic murine cerebral wall. *J. Neurosci.* 15, 6046–6057.
- Takahashi, T., Nowakowski, R.S., and Caviness, V.S., Jr. (1996). Interkinetic and migratory behavior of a cohort of neocortical neurons arising in the early embryonic murine cerebral wall. *J. Neurosci.* 16, 5762–5776.
- Yamashita, Y.M., Jones, D.L., and Fuller, M.T. (2003). Orientation of asymmetric stem cell division by the APC tumor suppressor and centrosome. *Science* 301, 1547–1550.
- Yoshida, A., Kobayashi, K., Many, H., Taniguchi, K., Kano, H., Mizuno, M., Inazu, T., Mitsuhashi, H., Takahashi, S., Takeuchi, M., et al. (2001). Muscular dystrophy and neuronal migration disorder caused by mutations in a glycosyltransferase, POMGnT1. *Dev. Cell* 1, 717–724.
- Zhong, W., Feder, J.N., Jiang, M.M., Jan, L.Y., and Jan, Y.N. (1996). Asymmetric localization of a mammalian numb homolog during mouse cortical neurogenesis. *Neuron* 17, 43–53.